In vitro analysis of carotid lesions using a preliminary microwave sensor to detect vulnerable plaques: Correlation with histology, Duplex ultrasound examination, and computed tomography scanner: The Imaging and Microwave Phenotyping Assessment of Carotid stenosis Threat (IMPACT) study

Rania Shahbaz, PhD,[a] Etienne Charpentier, MD,[b] Maharajah Ponnaiah, PhD,[c] Frédérique Deshours, PhD,[a] Hamid Kokabi, PhD,[a] Isabelle Brochériou, MD, PhD,[d] Gilles Le Naour, PhD,[a] Alban Redheuil, MD, PhD,[b] Fabien Koskas, MD, PhD,[e] *and* Jean-Michel Davaine, MD, PhD,[d,e] *Paris, France*

ABSTRACT

Objective: Progress in best medical treatment have made identification of best candidates for carotid surgery more difficult. New diagnostic modalities could be helpful in this perspective. Microwaves (MWs) can quantify dielectric properties (complex relative permittivity) of biological tissues and MW technology has emerged as a promising field of research for distinguishing abnormal tissues from healthy ones. We here evaluated the ability of a dedicated MW sensor developed in our laboratory to identify vulnerable carotid lesions.

Methods: We included 50 carotid lesions in this study. The plaques were analyzed and classified preoperatively by ultrasound (US) examination, computed tomography angiography and tested postoperatively using a MW sensor. Histopathological analysis was used as a gold standard to separate vulnerable plaques (VPs) from nonvulnerable plaques (NVPs).

Results: VPs were more frequently types 2 or 3 plaques (on US examination), had a greater proportion of low (<60 Hounsfield unit) and moderate (60-130 Hounsfield unit) attenuation components (computed tomography angiography) and displayed higher dielectric constant values (MW) than NVPs, which had an opposite profile. NVPs were more frequently asymptomatic plaques compared with VPs ($P = .035$). Multivariate analysis showed that US examination and MW identified VPs with a sensitivity of 77% and a specificity of 76% (cutoff value, −0.045; area under the curve, 0.848; $P < .0001$).

Conclusions: We found that the presence of types 2 to 3 (on US examination) and high dielectric constant plaques in vitro was highly indicative of a VP based on histological analysis. Further studies are needed to determine the potential of MW to identify the most dangerous asymptomatic carotid lesions. (JVS—Vascular Science 2024;5:100182.)

Keywords: Carotid plaque stability; Stroke; Microwave; Duplex US; Risk assessment

Surgery for asymptomatic carotid stenosis has become more and more controversial lately, in particular owing to major improvements in best medical treatment (BMT).[1,2] The main criterion that drives surgical indication is the degree of stenosis.[3-5] Decisions based solely on the degree of stenosis do not take into account the biological complexity of carotid atheromatous plaques.[6-8] Recent guidelines underline that efforts should be made to identify and integrate qualitative aspects of carotid lesions in the clinical decision.[9] The concept of vulnerable plaque (VP), inherited from the coronaries, applies to carotid lesions.[10] The composition of the plaque and its qualitative aspects are indeed critical regarding the risk of cerebrovascular events.[11,12] Calcification, inflammation, and intraplaque hemorrhage influence the plaque's mechanical behavior and its corresponding risk of rupture.[13,14] Histology has established that a thin fibrous cap, a lipid-rich necrotic core (LRNC) and an intraplaque hemorrhage (IPH) define a VP at risk of stroke[7,15-17]

To help better stratify a given carotid plaque risk of stroke, routine preoperative modalities are instrumental. Echogenicity and aspect of plaque surface have been identified as predictive factors of dangerous plaque with a good correlation with histology.[18] Ulceration, and, more recently, perivascular fat are promising

From the CNRS UMR8507, Laboratoire Génie Électrique et Électronique de Paris (GeePs),[a] Unité d'imagerie cardiovasculaire et thoracique, Hôpital La Pitié Salpêtrière (AP-HP), Laboratoire d'Imagerie Biomédicale, INSERM, CNRS, Institute of Cardiometabolism and Nutrition,[b] Sorbonne Université; IHU ICAN, Foundation for Innovation in Cardiometabolism and Nutrition, Pitié Salpêtrière Hospital[c]; Medicine Faculty, Sorbonne Université[d]; and the Department of Vascular and Endovascular Surgery, Pitié-Salpêtrière University Hospital.[e]

Correspondence: Jean-Michel Davaine, MD, PhD, Department of Vascular and Endovascular Surgery, Sorbonne Université, Pitie-Salpêtrière University Hospital, 47-83 Bd de l'Hôpital, Paris, France (e-mail: davainej@yahoo.fr).

The editors and reviewers of this article have no relevant financial relationships to disclose per the Journal policy that requires reviewers to decline review of any manuscript for which they may have a conflict of interest.

2666-3503

https://doi.org/10.1016/j.jvssci.2023.100182

indicators of carotid plaque threat on computed tomography (CT) scans.[19-21] However, very few studies have combined several routine modalities and compared them with clinical data and histology. As a result, we still lack a robust algorithm to support surgical decisions. Moreover, beyond current preoperative imaging modalities, developing new modalities capable of identifying risky plaques would be of great value. From this perspective, microwaves (MWs) have been getting much attention recently in the medical field. MW radiometry is able to detect small temperature changes in carotid plaques.[22] We here favored another property of MW, which are able to go through biological tissues. The resultant interaction between the electrical field and the medium is described by the complex relative permittivity which depends on the composition of each tissue.[23-26] MW imaging uses the natural dielectric contrast between healthy and abnormal tissues at the anatomical site of interest. We recently developed a MW sensor using the resonant method as a dielectric characterization technique to measure atherosclerotic plaques' dielectric properties.[27] To our knowledge, this report represents the first time such MW characterization has been used on carotid plaques. As a result, the goals of this study were to (i) describe carotid atheromatous plaques scheduled for surgery after a routine multimodal approach and (ii) assess the ability of our MW sensor to identify VPs.

ARTICLE HIGHLIGHTS

- **Type of Research:** Human in vitro study
- **Key Findings:** Fifty carotid plaques were analyzed using our microwave (MW) sensor. Vulnerable plaques based on histology analysis were significantly more likely to be types 2 or 3 on ultrasound examination and to have higher dielectric constant in MW compared with nonvulnerable plaques ($P < .0001$).
- **Take Home Message:** MW technology could be helpful in identifying the most dangerous asymptomatic carotid lesions.

METHODS

Patient characteristics. Indications for surgery followed guidelines on cerebrovascular disease.[9] Patients underwent Duplex ultrasound (US) imaging and CT angiography (CTA) preoperatively. Exclusion criteria consisted of prior carotid artery surgery or endovascular procedure of the same side or prior cervical radiation. Lesions were considered symptomatic if the patient had experienced a transient ischemic attack or stroke ipsilateral to the carotid lesion being studied within two months before surgery. The institutional review board at the Hôpitaux Universitaires Pitié Salpêtrière - Charles Foix approved the study, and patient consent was waived, given the nature of the study. Patient demographics and comorbidities were recorded at the time of enrolment. The use of antiplatelet agents, oral anticoagulant therapy, statins, and antihypertensive drugs was documented. In the case of asymptomatic carotid stenosis, the interval between the first surgical consultation and the operation was <6 weeks, whereas in the case of symptomatic carotid stenosis, this delay was <2 weeks.

Duplex US examination. The day before surgery, patients underwent a Duplex US examination performed by a certified vascular sonographer. Philips US system Affiniti 70, L12-5 50 mm Linear Probe transducer was used. The Grey-Weale updated scale[28-32] and color Doppler imaging were used to characterize the carotid plaque. Peak systolic and end-diastolic velocities, and internal carotid artery/common carotid artery ratio, were registered. The degree of stenosis was estimated using the North American Symptomatic Carotid Endarterectomy Trial criteria by comparing the diameter of the narrowest part of carotid artery to the diameter of the normal distal internal carotid artery. We particularly focused on diameter criteria to be consistent with CT scan analysis and to compare the two modalities. Images were documented in DICOM format and stored for later analyses.

CTA. In the 2 months before surgery, included patients underwent a ≥64 detector row CT scan covering the aortic arch to the cranioencephalic region. A 50- to 100-mL contrast medium with a flow rate of 3 to 5 mL/s was injected. CTA technical parameters included the following: a collimation of 0.6 × 0.6 mm, a slice thickness reconstruction of 0.6 mm, and a matrix size of 512 × 512. The C-filter algorithm of reconstruction was applied. A senior radiologist specialized in cardiovascular imaging (10 years of experience) reviewed all carotid arteries without knowing the operated side (right or left carotid artery). The carotid artery stenosis was assessed using the North American Symptomatic Carotid Endarterectomy Trial method.

Plaque ulceration was noted according to its width (≥5 mm).[33] Plaque analysis quantification was performed with a commercially dedicated software (iNtuition, TeraRecon, Inc., Foster City, CA). This solution semiautomatically quantifies three volumes for all carotid arteries: lumen volume, plaque volume, and total volume in cubic centimeters. Then, Hounsfield unit (HU) thresholds[20] defined the three major components of the plaque: fibrofatty (<60 HU), fibrotic (60-130 HU), and calcified (>130 HU) to compute each volume in cubic centimeters. The relative proportion of each plaque component was measured as the percentage of the plaque volume to normalize these volumes. Also, two regions of interest of 2.5 cm^2 were manually traced for each patient in the perivascular fat in the axial plane at the site of maximal stenosis. As previously published,[34-36] this parameter is called perivascular fat attenuation (PVFA).

Carotid endarterectomy. Patients were operated on under general anesthesia. Eversion carotid endarterectomy was performed to extract carotid plaque as a single specimen, then cut by the vascular surgeon into two identical samples longitudinally. One specimen was immersed in formol 4% and sent for histological analysis; the second was preserved in saline for MW analysis.

Histology. An experienced histopathologist (blind to the clinical details and other modalities results) conducted the histopathological analysis of the carotid plaques. The specimens were fixed in 10% buffered formalin before being decalcified with a Surgipath Decalcifier II (Leica Biosystems, Danvers, MA) solution and then embedded in paraffin. The histological slices were cut into a thickness of 3 microns and stained afterwards using an automated slide stainer and film cover slipper (Tissue-Tek, Sakura Finetek, Torrance, CA) by hematein, eosin, and saffron staining. A Nanozoomer Hamamatsu scanner was used to scan every slide's complete sectional area at 40× magnification with a resolution of 0.24 microns/pixel. The digital slides in NDPI format were later inspected on high-definition screens (Barco Coronis Fusion, Barco Inc, Duluth, GA) to determine the different tissue types. Whole sections were manually outlined using Viewer (NDP.view2 +) to achieve a well-defined mapping of each specimen component's area. This semiquantitative analysis was implemented to ascertain the presence of calcification, LRNC, IPH, and fibrous cap. Plaques with a LRNC, thin fibrous cap, and IPH were considered vulnerable.

MW. MW sensors use electromagnetic radiation to detect and measure various properties of objects or materials. The theory behind a MW sensor involves the transmission and reception of MW signals, which are then analyzed to extract information about the object being measured. Developing a MW sensor typically involves designing the transceiver system, selecting the appropriate frequency range, and optimizing the signal processing algorithms. The resonant technique is a widely used method in MW sensing, which involves measuring the resonant frequency of a resonant structure in response to changes in the environment or the material being measured. This technique is commonly used in the design of various types of MW sensors. A complementary split-ring resonator (CSRR) sensor was adopted in this specific application. The MW biosensor device developed in our laboratory is based on a CSRR structure designed on microstrip technology, as previously detailed.[27,37] Briefly, the resonant approach was agreed on to be used as it provides excellent sensitivity even when the analyzed materials have substantial dielectric losses. Thanks to its reduced dimensions, the planar sensor can characterize small samples of atheromatous plaques. The resonant frequency was chosen at around 2.4 GHz in the industrial, scientific, and medical radio frequency band for relatively good MW penetration into biological tissues and small dimensions of the sensor. The electromagnetic software High Frequency Structure Simulation Software from Ansys (Canonsburg, PA) was used to optimize the geometric parameters of the resonator and then to validate MW analysis. The received specimen is cautiously dried from the saline and then placed on the MW device. A standardized pressure was applied on plaques to ensure direct contact with the device and air elimination. MW measurements performed using a Rohde & Schwarz ZNB20 vector network analyzer and the complete set of scattering parameters (S-parameters) was registered vs frequency and was exploited via High Frequency Structure Simulation Software to extract dielectric parameters. At 2.2-GHz (ie the resonant frequency of the CSRR sensor), the dielectric constant of bone ($\varepsilon_r = 18$) was used as a reference for calcified plaques, and that of blood ($\varepsilon_r = 58$) was considered a cutoff point for plaques at risk.[38,39] The dielectric constant of blood, fat, and bones was proposed as a reference, even though, on a physiological level, the composition of atherosclerotic plaque is not essentially the same as those tissues. The reason these references were chosen is that they have been studied and documented already in international databases, whereas the dielectric constant of atheromatous plaque was never measured and it is always heterogeneous. Moreover, high permittivity is characteristic of tissues rich in polar molecules, especially water, whereas low permittivity is typical of tissues rich in nonpolar elements, such as adipose tissue. Tissue characteristics must be understood first for diagnostic imaging to establish whether a contrast exists between the background tissue and the tissue of interest. In particular, the blood value was used as a surrogate for intraplaque hemorrhage.

Statistical analyses. Continuous variables were summarized using mean ± standard deviation and categorical variables as frequency (percentage). We performed a two-sided Mann-Whitney *U* test for continuous variables and χ^2 for categorical variables. A variable is significant when the *P* value is ≤.05. Multivariable analysis were performed by logistic regression method. Variable selection was made by backward conditional method. Variables selection were chosen a priori based on scientific evidence. The models were validated by goodness of the overall fit of the models at the 5% level significance and receiving operating characteristic (ROC) curve analysis. Coefficients of the logistic regression were calculated to develop the multimodal prognostic score. The cutoff threshold was chosen with 77% and 70% of sensitivity and specificity, respectively for an area under the curve (AUC) of 0.8. All the statistical analysis were performed using SPSS v.28 statistical software (IBM, Chicago, IL).

Table I. Baseline characteristics of 49 patients with or without symptoms before carotid endarterectomy

	Total (n = 50)	Asymptomatic (n = 35)	Symptomatic (n = 15)	*P* value
Total No. of plaques	50 (100)	35 (70)	15 (30)	
Mean age, years	73 ± 8.8	73.6	72.4	.135
Body mass index, kg/m^2	25.1 ± 3.4			
Female sex	14 (28)	11 (31)	3 (20)	
Arterial hypertension	37 (74)	26 (74)	11 (73)	.774
Smoking				.589
Active	8 (16)	6 (17)	2 (13)	
Previous	18 (36)	11 (31)	7 (47)	
Diabetes	13 (26)	7 (20)	6 (40)	.140
Dyslipidemia	31 (62)	21 (60)	10 (67)	.656
Obesity	3 (6)	3 (9)	0	
Cardiovascular disease	23 (46)	16 (46)	7 (47)	
Peripheral arterial disease	12 (24)	9 (26)	3 (20)	
History of stroke/TIA	19 (38)	9 (26)	10 (67)	
Antiplatelet drug	35 (70)	28 (80)	7 (47)	
Vitamin K Antagonists	1 (2)	1 (3)	0	
Novel Oral anticoagulant	3 (6)	2 (6)	1 (7)	
2 antiplatelet drugs	9 (18)	7 (20)	2 (13)	
Beta-blockers	22 (44)	15 (43)	7 (47)	
Statin	43 (86)	32 (91)	11 (73)	
Diuretics	9 (18)	7 (20)	2 (13)	
Angiotensin II receptor blockers	16 (32)	11 (31)	5 (33)	
Angiotensin-converting enzyme	18 (36)	16 (46)	2 (13)	
Calcium channel blockers	22 (44)	16 (46)	6 (40)	

TIA, Transient ischemic attack.
Data are presented as number (%) or mean ± standard deviation.

Table II. Composition of the plaques in the vulnerable plaque (*VP*) vs nonvulnerable plaque (*NVP*) groups and symptomatic vs asymptomatic group

	All	VP (n = 22)	NVP (n = 28)	*P* value	Symptomatic (n = 15)	Asymptomatic (n = 35)	*P* value
% Fibrous cap	55.1 ± 17	41.9 ± 11	65.4 ± 15	.000	47.5 ± 13	58.3 ± 18	.043
% LRNC	25.3 ± 21	45.7 ± 11	9.3 ± 9	.000	32.2 ± 20	22.4 ± 20	.133
% Calcification	8.5 ± 12	3.0 ± 3	12.8 ± 15	.010	12.5 ± 15	6.8 ± 10	.074
Symptomatic (n = 15)		10 (46)	5 (18)	.035			
Asymptomatic (n = 35)		12 (54)	23 (82)				

LRNC, Lipid-rich necrotic core; *NVP*, nonvulnerable plaque; *VP*, vulnerable plaque.
Data are presented as mean ± standard deviation or number (%).

RESULTS

Patients. Overall, 50 carotid specimens (49 patients) were included between January 2020 and October 2022. The mean age was 73± 9 years, primarily male patients (72%) (Table I). Patients were considered for surgery in case of stenosis of >70%, or between 60% and 70% for symptomatic lesions or in case of asymptomatic lesion presenting features of instability according to the referral surgeon (ulceration, soft irregular plaque, between 60% and 70% of stenosis in CTA but high velocities on US examination) (Table II).

Thirty-one of the 49 patients had BMT (1 or 2 antiplatelet agents, statins, and antihypertensive drugs). Among the 31 BMT+ patients, 13 (42%) had a VP based on histology analysis, compared with 9 of the 18 patients in the BMT group ($P = .3$). The surgical site was on the right side in one-half of the cases. The median length of hospitalisation was 3 days. One postoperative transient ischemic

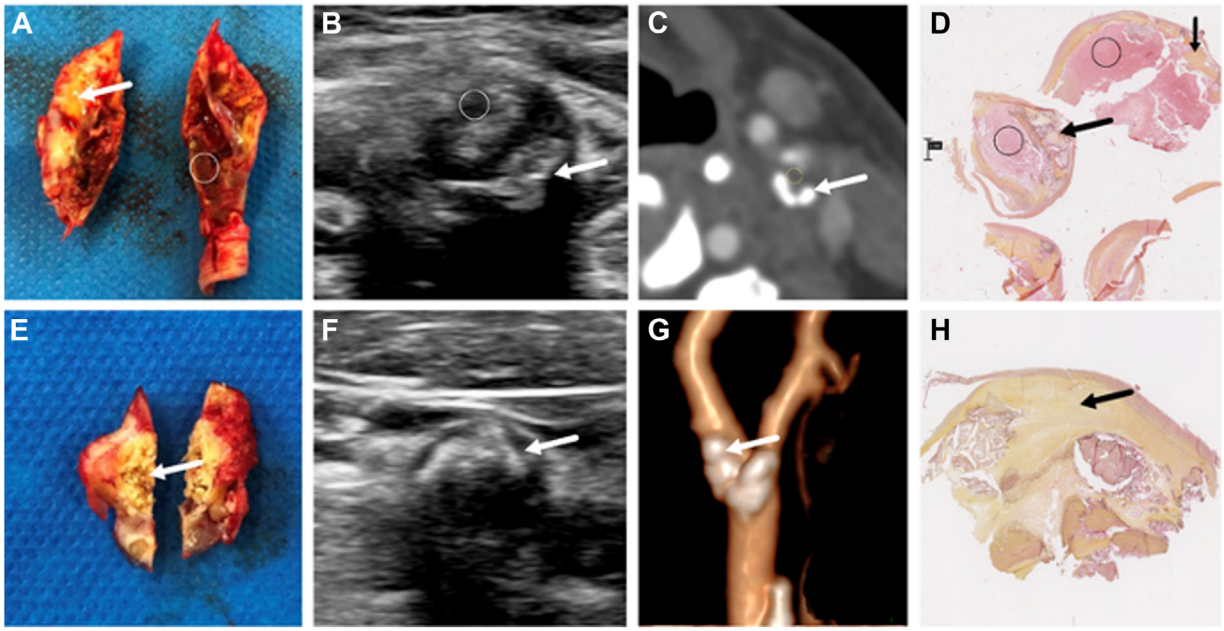

Fig 1. Representative illustration of multimodal assessment of vulnerable plaques (VPs) **(A-D)** and nonvulnerable plaques (NVPs) **(E-H)**. The VP in (A) shows similar findings between the in vivo examination of duplex ultrasound (DUS) examination and computed tomography (CT) scan **(B, C)**, respectively, and the histological analysis in **(D)**. Similarly, the NVP in (E) displays comparable findings between the in vivo assessment of DUS examination and CT scan **(F, G)**, respectively, and the histological analysis in **(H)**.

Table III. Distribution of the lesions according to symptoms, degree of stenosis, and vulnerability status in histology

			NASCET 60%-69%		NASCET 70%- 79%		NASCET 80%- 90%	
	VP	NVP	VP	NVP	VP	NVP	VP	NVP
Symptomatic (n = 15)	10 (46)	5 (18)	0	3	4	1	6	1
Asymptomatic (n = 35)	12 (54)	23 (82)	3	9	6	5	3	9

NASCET, North American Symptomatic Carotid Endarterectomy Trial; *NVP*, nonvulnerable plaque; *VP*, vulnerable plaque.
Values are number (%).

attack was observed; there were no adverse cardiovascular events and no deaths.

Multimodality-based characterization of carotid plaques. Histology identified 22 VPs. Quantitatively, these VPs had a large content of lipidic-necrotic material (45%) and a low amount of calcification (3%) and fibrosis (41%) as opposed to nonvulnerable plaques (NVPs), which were less lipidic necrotic (9%) and more calcified (13%) and fibrotic (65%) ($P < .05$) (Table II and Fig 1). Consistently, NVPs were more frequently asymptomatic (23/35) lesions ($P < .035$) (Table III).

Duplex US analysis showed that 78% of VPs were type 2 to 3 plaques according to the Gray-Weale scale, as opposed to NVPs that mainly were type 4 and 5 plaques. Also, the amount of necrosis significantly decreased ($P = .010$) and the amount of calcification significantly increased ($P = .033$) from type 2 to type 5 lesions (Fig 2, *A-C*).

ROC curve analysis showed that a cutoff of 17% of necrosis (sensitivity, 70%; specificity, 70%; $P = .003$) and 4.2% of calcification (sensitivity, 65%; specificity, 70%; $P = .021$) distinguished type 2 and 3 from type 4 and 5 plaques (Fig 2, *a-c*).

The CTA analysis found no difference in terms of HU pattern between symptomatic and asymptomatic plaques, nor between VPs and NVPs (Supplementary Fig 1). In contrast, type 2 and 3 plaques had significantly more HU of <60 and significantly more HU between 60 and 130 than type 4 and 5 plaques ($P = .035$ and $P = .038$, respectively) (Fig 3). PVFA values were not significantly different between symptomatic, asymptomatic, VPs, NVPs and between type 2 and 3 and type 4 and 5 plaques (Supplementary Fig 2).

MW device ability to identify VP in vitro. The constant dielectric significantly decreased from type 2 to type 5

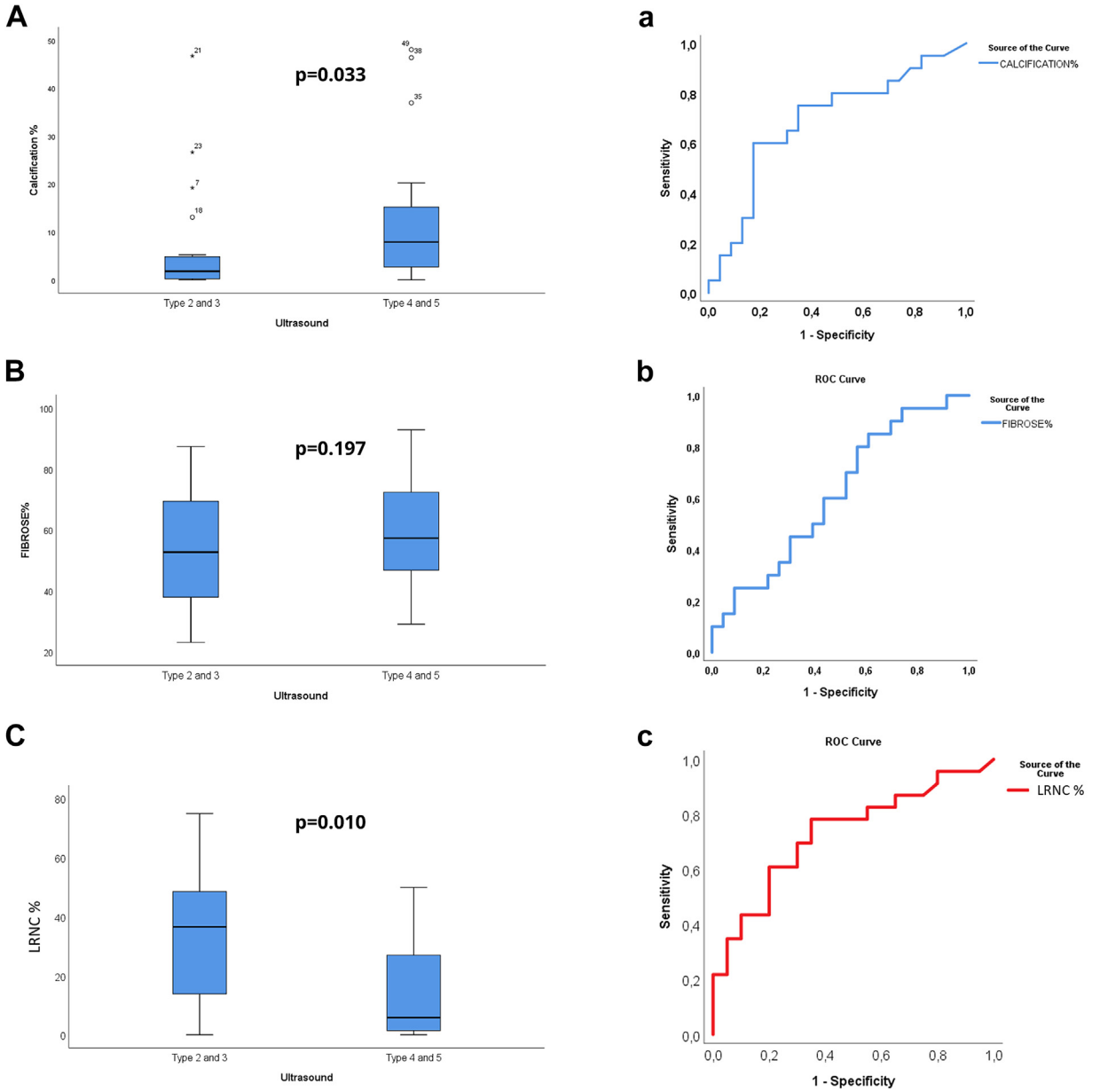

Fig 2. Statistical analysis of the relationship between histology and duplex ultrasound (DUS) examination. The degree of calcification was higher **(A)** and the lipid-rich necrotic core (LRNC) amount lower **(C)** in type 4/5 plaques based on the Grey-Weale updated scale classification. No significant difference was noted in terms of fibrosis **(B)**. Receiving operating characteristic (ROC) curve analysis found that a cutoff of 17% of necrosis (sensitivity, 70%; specificity, 70%; $P = .003$) and 4.2% of calcification (sensitivity, 65%; specificity, 70%; $P = .021$) distinguished type 2/3 from type 4/5 plaques **(A-C)**.

plaques (Fig 4, *A*) ($P = .004$). ROC curve analysis showed a good dielectric constant (AUC, 0.761) ability to predict type 2 and 3 plaques (cutoff value, 18.75; sensitivity, 73%; sensibility, 80%; $P = .001$) (Fig 4, *a*).

Multivariate analysis showed that constant dielectric ($P = .033$) combined with type 2 and 3 Duplex US plaque ($P = .011$) were predictive characteristics of VPs (Fig 4, *B*). Using these variables, we apply a multimodal prognostic score able to significantly predict the presence of a VP by applying the equation: score = 1.760 + (−0.062 × constant dielectric) + (−3.367 × Gray-Weale classification 2 and 3 or 4 and 5) (cutoff value, −0.045;

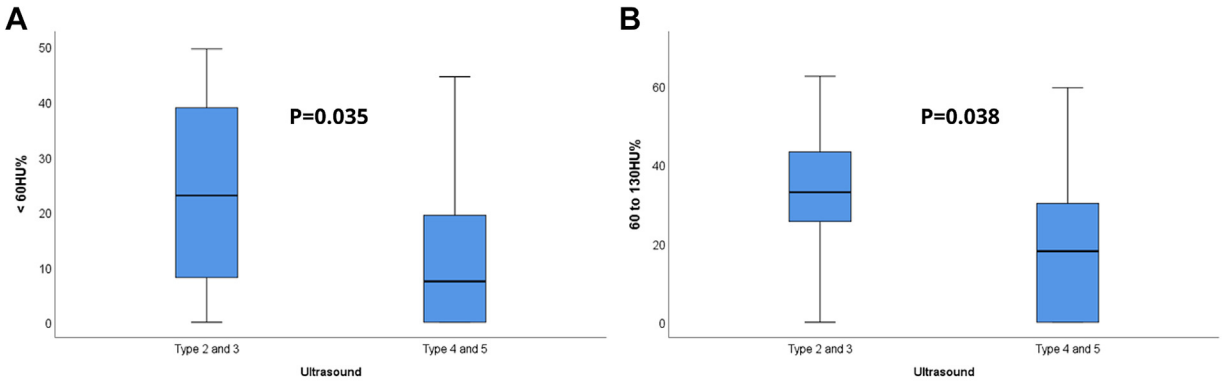

Fig 3. Association between computed tomography (CT) scan and duplex ultrasound (DUS) examination. Box plot analysis of Hounsfield unit (*HU*) groups vs Gray-Weale scale groups in DUS examination showing no significant association between CT scan results and DUS analysis.

AUC, 0.848; sensitivity, 77%; specificity, 76%; $P < .0001$) (Fig 4, *b*).

DISCUSSION

Multimodal characterization of carotid plaques has rarely been performed. Most available studies compare two different modalities among Duplex-US, CTA, and histology.[40,41,42] Here, we performed a systematic longitudinal assessment of each plaque with routine modalities: clinical presentation, Duplex-US, CTA, and MW analysis, and compared it with histology, the latter being usually considered as the gold standard to identify VPs prone to rupture.[10] We confirmed here that VPs had a higher lipidic and necrotic content and were poorly calcified, whereas NVPs were less lipidic and more fibrocalcic. Also, NVPs were found to be significantly associated with asymptomatic nature of carotid plaques, further supporting the accuracy of histology to identify the nature of carotid plaques. In contrast with previous studies wherein a content of 30% to 40% necrosis was used to define a LRNC,[39,43] here we observed thresholds of 17% of necrosis and 4% of calcification in VPs. The Gray-Weale scale results were consistent with histology and symptoms The updated Gray-Weale scale classifies plaques according to their echogenicity and has proven reliable and reproducible.[31,41,44] Previous works have also shown a good correlation between the Gray-Weale scale and symptoms[45] and histology with type 1 and 2 plaques being VPs.[32] As a result, a more detailed analysis on Duplex US examination should be encouraged, beyond the degree of stenosis and velocity measurements, and the Gray-Weale scale should be part of the routine Duplex US report. CTA indicates plaque composition with fatty, fibrotic, and calcified plaques displaying different values of HUs.[46,47] Fatty plaques are associated with a higher risk of stroke than calcified plaques.[9,48,49] The present work adds up to previous studies and altogether, these data may help to better characterize the relationship between histology and routine preoperative modalities, which could be critical to improve surgical screening of carotid lesions. We also studied the significance of PVFA on CTA. Increased density of PVF has been suggested to correlate with histopathological markers of inflammation, such as inflammatory cytokines and macrophages and it seems that a significant increase in PVFA is observed in symptomatic compared with asymptomatic carotids.[34-36,50,51] We observed here an opposite pattern with lower PVFA values in symptomatic and VPs as opposed to asymptomatic and NVPs. The previous studies were retrospective, used different protocol analyses, and had no histopathological controls. In addition, the absolute values of PVFA differ widely from one study to another, limiting the comparability. Our findings may differ owing to the limited number of patients or to a difference in our protocol. Dedicated studies are warranted to determine the prognostic value of carotid PVFA.

Improving the screening of patient for carotid surgery is necessary. This is the purpose of our MW device. Previous studies on the carotid artery using MW were based on MW radiometry. The principle was to detect temperature changes in human tissues with high accuracy. Such measures give an indirect idea of carotid plaque inflammation.[22] Here, we used MW imaging with a different approach. We analyzed in vitro the signal reflected by our sample, which differed according to plaque composition. At this bandwidth, the technology is harmless. The ability of our device to identify VPs in vitro seems promising and further studies are underway to evaluate its potential in vivo. Ultimately, a transcutaneous MW sensor could be helpful in decision-making. However, additional development of MW sensor technology is required to make possible a more accurate characterization of plaque and to transform the device into a diagnostic tool that medical practitioners can use. Independent verification of the depth of the electrical field penetration is

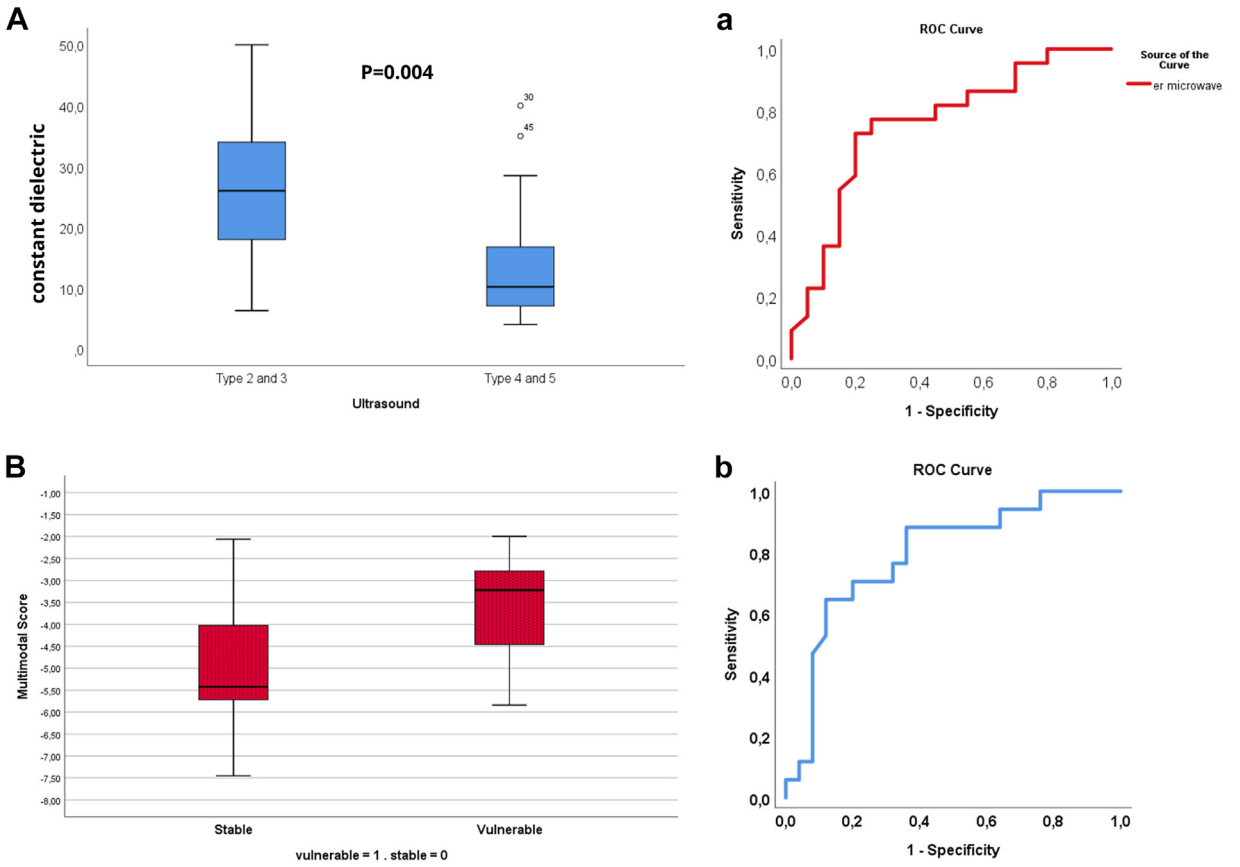

Test Result Variable(s)	Area	95% Confidence Interval		pvalue
		Lower Bound	Upper Bound	
Multimodal Score	0.8001	0.65	0.93	4.2672E-05

Cutoff -4.50, Sensitivity = 77%, Specificity = 70%

Fig 4. Microwave (MW) and multimodal assessment of carotid vulnerable plaques (VPs). Whisker chart and receiving operating characteristic (ROC) curve statistical analysis of the constant dielectric vs echogenicity types **(A and a)** and multimodal prognostic score aiming at predicting the vulnerability of carotid plaques (**B, b** and table). The constant dielectric significantly decreased from type 2 to type 5 plaques ($P = .004$) (area under the curve [AUC], 0.76; cutoff value, 18.75; sensitivity, 73%; specificity, 80%; $P = .00$). Constant dielectric c ($P = .033$) combined with type 2/3 plaque on duplex ultrasound (DUS) examination ($P = .011$) are predictive of VPs: score = 1.760 + (−0.062 × constant dielectric) + (−3.367 × Gray-Weale scale classification 23 or 45) (cutoff value, −0.045; AUC, 0.848; sensitivity, 77%; specificity, 76%; $P < .0001$).

required; depending on the findings, the design or the frequency may need to be adjusted. Further, the upgraded sensor that will be chosen needs to be validated by being tested on a large number of ex vivo samples and phantoms. The findings of these measurements need to be reproducible and consistent so they can be used as a benchmark for the sensitivity and specificity when compared with the measurements that will be done in vivo. Because no single modality is able to determine with certainty which patient should proceed to surgery, we hypothesize that combining the results of several modalities could improve our ability to detect the most dangerous lesions. Our importantly multimodal prognostic score showed that using dielectric constant combined with Grey-Weale scale results led to identification of a VP with 77% and 70% of sensitivity and specificity (AUC, 0.8).

Only two-third of patients were under BMT upon meeting their vascular surgeon, that is, after one or several medical consultations. Whether the lack of observance is an argument in favor of surgery is debatable and beyond the scope of this study; however, one has to acknowledge that it is a reality that should be taken into consideration.

This study has several limitations. Its modest number of patients limits the significance of our results. During the surgery, the plaque was cut symmetrically along a longitudinal axis in two pieces (one for MW, the other for

histology analysis). However, we cannot exclude some regional differences between samples, which may have affected the results. Our MW device was tested ex vitro and its benefit has to be confirmed in vivo. Our equation suggests that evaluation of carotid lesions with MW could improve the screening of patients who are good candidates for surgery. However, the results were obtained postoperatively on plaque specimen; thus, the equation is of no clinical usefulness at this stage. A percutaneous device to assess MW properties of plaques preoperatively has to be developed. We have not used magnetic resonance imaging because it is not part of our routine preoperative workup. However, magnetic resonance imaging data would have strengthened our analyses.

CONCLUSIONS

This prospective work showed that types 2 and 3 plaques according to Gray-Weale scale and high dielectric constant plaques based on MW analysis are associated significantly with a vulnerable phenotype in histology. The combination of US and MW analyses was more efficient in identifying VPs than a single modality analysis, suggesting that more studies using a multimodal approach could improve the screening of asymptomatic patients for carotid surgery.

AUTHOR CONTRIBUTIONS

Conception and design: RS, FD, HK, IB, AR, FK, JD
Analysis and interpretation: RS, EC, FD, IB, GN, AR, JD
Data collection: RS, EC, MP, FD, HK, IB, JD
Writing the article: RS, EC, MP, FD, JD
Critical revision of the article: RS, FD, HK, IB, GN, AR, FK, JD
Final approval of the article: RS, EC, MP, FD, HK, IB, GN, AR, FK, JD
Statistical analysis: RS, MP, JD
Obtained funding: Not applicable
Overall responsibility: JD

DISCLOSURES

None.

REFERENCES

1. Reiff T, Eckstein HH, Mansmann U, et al. Carotid endarterectomy or stenting or best medical treatment alone for moderate-to-severe asymptomatic carotid artery stenosis: 5-year results of a multicentre, randomised controlled trial. *Lancet Neurol*. 2022;21:877—888.
2. Arasu R, Arasu A, Muller J. AJGP-11-2021-Clinical-Arasu-Carotid-Artery-Stenosis-WEB 2021;. 2021;50(11):821—825.
3. Wardlaw J, Chappell F, Best J, Wartolowska K, Berry E. Non-invasive imaging compared with intra-arterial angiography in the diagnosis of symptomatic carotid stenosis: a meta-analysis. *Lancet*. 2006;367:1503—1512.
4. Goldstein LB, Hasselblad V, Matchar DB, McCrory DC. Comparison and meta-analysis of randomized trials of endarterectomy for symptomatic carotid artery stenosis. *Neurology*. 1995;45:1965—1970.
5. Meershoek AJA, de Vries EE, Veen D, et al. Meta-analysis of the outcomes of treatment of internal carotid artery near occlusion. *Br J Surg*. 2019;106:665—671.
6. Coscas R, Rhissassi B, Gruet-Coquet N, et al. Open surgery remains a valid option for the treatment of recurrent carotid stenosis. *J Vasc Surg*. 2010;51:1124—1132.
7. Saba L, Micheletti G, Brinjikji W, et al. Carotid intraplaque-hemorrhage volume and its association with cerebrovascular events. *Am J Neuroradiol*. 2019;40:1731—1737.
8. Zhu G, Hom J, Li Y, et al. Carotid plaque imaging and the risk of atherosclerotic cardiovascular disease. *Cardiovasc Diagn Ther*. 2020;10:1048.
9. Naylor R, Rantner B, Ancetti S, et al. Editor's choice — European Society for vascular surgery (ESVS) 2023 clinical practice guidelines on the management of atherosclerotic carotid and vertebral artery disease. *Eur J Vasc Endovasc Surg*. 2023;65:7—111.
10. Finn AV, Nakano M, Narula J, Kolodgie FD, Virmani R. Concept of vulnerable/unstable plaque. *Arterioscler Thromb Vasc Biol*. 2010;30:1282—1292.
11. Larson AS, Brinjikji W, Savastano L, et al. Carotid intraplaque hemorrhage and stenosis: at what stage of plaque progression does intraplaque hemorrhage occur, and when is it most likely to be associated with symptoms? *Am J Neuroradiol*. 2021;42:1285—1290.
12. Hetterich H, Fill S, Herzen J, et al. Grating-based X-ray phase-contrast tomography of atherosclerotic plaque at high photon energies. *Zeitschrift fur Medizinische Physik*. 2013;23:194—203.
13. Davaine JM, Quillard T, Brion R, et al. Osteoprotegerin, pericytes and bone-like vascular calcification are associated with carotid plaque stability. *PLoS ONE*. 2014;9:e107642.
14. Paraskevas KI, Veith FJ, Spence JD. How to identify which patients with asymptomatic carotid stenosis could benefit from endarterectomy or stenting. *Stroke Vasc Neurol*. 2018;3:92—100.
15. Hishikawa T, Iihara K, Yamada N, Ishibashi-Ueda H, Miyamoto S. Assessment of necrotic core with intraplaque hemorrhage in atherosclerotic carotid artery plaque by MR imaging with 3D gradient-echo sequence in patients with high-grade stenosis: clinical article. *J Neurosurg*. 2010;113:890—896.
16. Heymann MF, Herisson F, Davaine JM, et al. Role of the OPG/RANK/RANKL triad in calcifications of the atheromatous plaques: comparison between carotid and femoral beds. *Cytokine*. 2012;58:300—306.
17. Funaki T, Iihara K, Miyamoto S, et al. Histologic characterization of mobile and nonmobile carotid plaques detected with ultrasound imaging. *J Vasc Surg*. 2011;53:977—983.
18. Sztajzel R. Ultrasonographic assessment of the morphological characteristics of the carotid plaque. *Swiss Med Wkly*. 2005;135:635—643.
19. Choi E, Byun E, Kwon SU, et al. Carotid plaque composition assessed by CT predicts subsequent cardiovascular events among subjects with carotid stenosis. *Am J Neuroradiol*. 2021;42:2199—2206.
20. Weert TT, Monyé C, Meijering E, et al. Assessment of atherosclerotic carotid plaque volume with multidetector computed tomography angiography. *Int J Cardiovasc Imag*. 2008;24:751—759.
21. Oikonomou EK, Marwan M, Desai MY, et al. Non-invasive detection of coronary inflammation using computed tomography and prediction of residual cardiovascular risk (the CRISP CT study): a post-hoc analysis of prospective outcome data. *Lancet*. 2018;392:929—939.
22. Drakopoulou M, Moldovan C, Toutouzas K, Tousoulis D. The role of microwave radiometry in carotid artery disease. Diagnostic and clinical prospective. *Curr Opin Pharmacol*. 2018;39:99—104.
23. Sterzer F. Microwave medical devices. *IEEE Microw Mag*. 2002;3:65—70.
24. Kozhemyakin Y, Rehault-Godbert S, Dubuc D, Grenier K. *Millifluidic Sensor Designed to Perform the Microwave Dielectric Spectroscopy of Biological Liquids*. 2022 52nd European Microwave Conference, EuMC; 2022:412—415.
25. Maffongelli M, Poretti S, Salvadè A, et al. *Design and Experimental Test of a Microwave System for Quantitative Biomedical Imaging*. MeMeA 2018 - 2018 IEEE International Symposium on Medical Measurements and Applications, Proceedings; 2018:2—7.
26. Persson M, Fhager A, Trefna HD, et al. Microwave-based stroke diagnosis making global prehospital thrombolytic treatment possible. *IEEE (Inst Electr Electron Eng) Trans Biomed Eng*. 2014;61:2806—2817.
27. Shahbaz R, Deshours F, Alquie G, et al. Identification of carotid plaques composition through a compact CSRR-based microwave sensor. *IRBM*. 2022;44:100734.

28. De Waard DD, Morris D, De Borst GJ, Bulbulia R, Halliday A. Asymptomatic carotid artery stenosis: who should be screened, who should be treated and how should we treat them? *J Cardiovasc Surg*. 2017;58:3–12.
29. Elatrozy T, Nicolaides A, Tegos T, Griffin M. The objective characterisation of ultrasonic carotid plaque features. *Eur J Vasc Endovasc Surg*. 1998;16:223–230.
30. Saba L, Sanfilippo R, Montisci R, Atzeni M, Ribuffo D, Mallarini G. Vulnerable plaque: detection of agreement between multi-detector-row CT angiography and US-ECD. *Eur J Radiol*. 2011;77:509–515.
31. Tahmasebpour HR, Buckley AR, Cooperberg PL, Fix CH. Sonographic examination of the carotid Arteries1. *Radiographics*. 2005;25:1561–1575.
32. Casadei A, Floreani M, Catalini R, Serra C, Assanti AP, Conci P. Sonographic characteristics of carotid artery plaques: implications for follow-up planning? *Journal of ultrasound*. 2012;15:151–157.
33. Hermus L, van Dam GM, Zeebregts CJ. Advanced carotid plaque imaging. *Eur J Vasc Endovasc Surg*. 2010;39:125–133.
34. Antonopoulos AS, Sanna F, Sabharwal N, et al. Detecting human coronary inflammation by imaging perivascular fat. *Sci transl med*. 2017;9:eaal2658.
35. Baradaran H, Myneni PK, Patel P, et al. Association between carotid artery perivascular fat density and cerebrovascular ischemic events. *J Am Heart Assoc*. 2018;7:e010383.
36. Chatterjee D, Shou BL, Matheson MB, et al. Perivascular fat attenuation for predicting adverse cardiac events in stable patients undergoing invasive coronary angiography. *J Cardiovasc Comput Tomogr*. 2022;16:483–490.
37. Shahbaz R, Deshours F, Alquié G, et al. Diagnosis of atheromatous carotid plaque: dielectric constant measurement using microwave resonant technique versus ultrasound B-mode images. In: *2021 USNC-URSI radio science meeting (USCN-URSI RSM)*. 2021:40–44.
38. Gabriel C, Gabriel S, Corthout E. The dielectric properties of biological tissues: I. Literature survey. *Phys Med Biol*. 1996;41:2231–2249.
39. Gabriel S, Lau RW, Gabriel C. The dielectric properties of biological tissues: III. Parametric models for the dielectric spectrum of tissues. *Phys Med Biol*. 1996;41:2271–2293.
40. Watanabe Y, Nagayama M, Suga T, et al. Characterization of atherosclerotic plaque of carotid arteries with histopathological correlation: vascular wall MR imaging vs. color Doppler ultrasonography (US). *J Magn Reson Imag*. 2008;28:478–485.
41. Saba L, Anzidei M, Marincola BC, et al. Imaging of the carotid artery vulnerable plaque. *Cardiovasc Intervent Radiol*. 2014;37:572–585.
42. Diab HMH, Rasmussen LM, Duvnjak S, Diederichsen A, Jensen PS, Lindholt JS. Computed tomography scan based prediction of the vulnerable carotid plaque. *BMC Med Imaging*. 2017;17:61.
43. Cademartiri F, Balestrieri A, Cau R, et al. Insight from imaging on plaque vulnerability: similarities and differences between coronary and carotid arteries—implications for systemic therapies. *Cardiovasc Diagn Ther*. 2020;10:1150–1162.
44. Rafailidis V, Chryssogonidis I, Tegos T, Kouskouras K, Charitanti-Kouridou A. Imaging of the ulcerated carotid atherosclerotic plaque: a review of the literature. *Insights Imaging*. 2017;8:213–225.
45. Geroulakos G, Ramaswami G, Nicolaides A, et al. Characterization of symptomatic and asymptomatic carotid plaques using high-resolution real-time ultrasonography. *Br J Surg*. 1993;80:1274–1277.
46. Saba L, Sanfilippo R, Balestrieri A, et al. Relationship between carotid computed tomography dual-energy and brain leukoaraiosis. *J Stroke Cerebrovasc Dis*. 2017;26:1824–1830.
47. Kristanto W, van Ooijen PMA, Jansen-van der Weide MC, Vliegenthart R, Oudkerk M. A meta analysis and hierarchical classification of HU-based atherosclerotic plaque characterization criteria. *PLoS One*. 2013;8:1–13.
48. Mitchell CC, Stein JH, Cook TD, et al. Histopathologic validation of grayscale carotid plaque characteristics related to plaque vulnerability. *Ultrasound med biol*. 2017;43:129–137.
49. Karlöf E, Buckler A, Liljeqvist ML, et al. Carotid plaque phenotyping by correlating plaque morphology from computed tomography angiography with transcriptional profiling. *Eur J Vasc Endovasc Surg*. 2021;62:716–726.
50. Zhang S, Yu X, Gu H, Kang B, Guo N, Wang X. Identification of high-risk carotid plaque by using carotid perivascular fat density on computed tomography angiography. *Eur J radiol*. 2022;150:110269.
51. Sun JT, Sheng XC, Feng Q, et al. Pericoronary fat attenuation index is associated with vulnerable plaque components and local immune-inflammatory activation in patients with non-ST elevation acute coronary syndrome. *J Am Heart Assoc*. 2022;11:e022879.

Submitted Aug 8, 2023; accepted Nov 3, 2023.